Res Chem Intermed (2015) 41:913–925
DOI 10.1007/s11164-013-1244-7

Investigation of inhibition by 6-bromo-3-nitroso-2-phenylimidazol[1,2-α]pyridine of the corrosion of C38 steel in 1 M HCl

Ali Anejjar · Rachid Salghi · Abdelkader Zarrouk · Hassan Zarrok · Omar Benali · Belkheir Hammouti · Salem Selim Al-Deyab · Nour-Eddine Benchat · Rafik Saddik

Received: 19 February 2013 / Accepted: 26 April 2013 / Published online: 16 May 2013
© Springer Science+Business Media Dordrecht 2013

Abstract Inhibition of the corrosion of C38 steel in 1 M HCl by 6-bromo-3-nitroso-2-phenylimidazol[1,2-α]pyridine (BNPP) has been studied by use of electrochemical impedance spectroscopy and potentiodynamic polarization. BNPP inhibited the corrosion of C38 steel in 1 M HCl solution. Polarization curves show that BNPP acts as mixed-type inhibitor. Changes in impedance (charge-transfer resistance, R_t, and double layer capacitance, C_{dl}) were indicative of adsorption of BNPP on the metal surface, leading to formation of a protective film. The extent of surface coverage by the inhibitor was determined by measurement of weight loss; it was found that adsorption of this inhibitor on the C38 steel surface obeys the Langmuir adsorption isotherm. The effect of temperature on the corrosion behaviour was studied in the range 289–328 K. The results showed that the rate of corrosion of C38 steel increased with increasing temperature both in the presence of 10^{-3} M BNPP and in its absence. Activation energies in the presence and absence

A. Anejjar · R. Salghi (✉)
Laboratory of Environmental Engineering and Biotechnology, ENSA, Université Ibn Zohr, PO Box 1136, 80000 Agadir, Morocco
e-mail: r_salghi@yahoo.fr

A. Zarrouk · B. Hammouti · N.-E. Benchat · R. Saddik
LCAE-URAC 18, Faculty of Science, University of Mohammed Premier, Po Box 717, 60000 Oujda, Morocco

H. Zarrok
Laboratory Separation Processes, Faculty of Science, University Ibn Tofail, PO Box 242, Kenitra, Morocco

O. Benali
Department of Biology, Faculty of Sciences and Technology, Saïda University, Saïda, Algeria

S. S. Al-Deyab
Petrochemical Research Chair, Chemistry Department, College of Science, King Saud University, P.O. Box 2455, Riyadh 11451, Saudi Arabia

of BNPP were obtained by measuring the temperature dependence of charge-transfer resistance.

Keywords Corrosion · Inhibition · BNPP · C38 steel · HCl · Polarisation curves · EIS

Introduction

Mild steel is exposed to the action of acid in many industrial processes in which acid is used, for example in oil well acidification, acid pickling, acid cleaning, and acid descaling. Because the effects of exposure to acid can be extremely severe, corrosion inhibitors are widely used in industry to prevent or reduce rates of corrosion of metallic materials in these acid media. The use of inhibitors is one of the best methods of protecting metals against corrosion [1, 2]. Because of the aggressiveness of the acids, inhibitors are used to reduce the rate of dissolution of the metal [3–10]. The effect of organic nitrogen compounds on the corrosion behaviour of metallic materials in aggressive solutions has been well documented [11–27]. Choice of these is based on their stability as inhibitors of corrosion of metallic materials in acidic media. In this work, inhibition of the corrosion of C38 steel in 1 M HCl solution by 6-bromo-3-nitroso-2-phenylimidazol[1,2-α]pyridine (Fig. 1) was investigated by Tafel polarization, electrochemical impedance spectroscopy (EIS), and measurement of weight loss.

Materials and methods

Materials

The steel used in this study was a carbon steel (Euronorm: C35E carbon steel and US specification: SAE 1035) of chemical composition (wt%) of 0.370 % C, 0.230 % Si, 0.680 % Mn, 0.016 % S, 0.077 % Cr, 0.011 % Ti, 0.059 % Ni, 0.009 % Co, 0.160 % Cu, and the remainder iron (Fe). Before the experiments the C38 steel samples were pre-treated by grinding with emery paper SiC (120, 600, and 1200 grade), rinsing with distilled water, degreasing by immersion in acetone in an ultrasonic bath for 5 min, washing again with bidistilled water, and then drying at room temperature. The acid solutions (1.0 M HCl) were prepared by dilution of analytical reagent-grade 37 % HCl with double-distilled water. The range of concentration of 3-bromo-2-phenylimidazol[1,2-α]pyridine was 10^{-6} M to 10^{-3} M.

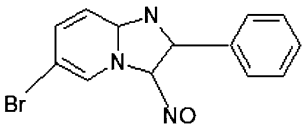

Fig. 1 The molecular structure of 6-bromo-3-nitroso-2-phenylimidazol[1,2-α]pyridine (BNPP)

Measurements

Weight loss measurements

Gravimetric measurements were performed after 6 h at room temperature, by use of an analytical balance (precision ± 0.1 mg). The C38 steel specimens used were rectangular in shape (length = 1.6 cm, width = 1.6 cm, thickness = 0.07 cm). Gravimetric experiments were performed in a double glass cell equipped with a thermostated cooling condenser containing 80 mL non-de-aerated test solution. After immersion, the C38 steel specimens were withdrawn, carefully rinsed with bidistilled water, cleaning ultrasonically in acetone, dried at room temperature, and then weighed. Triplicate experiments were performed in each case and the mean value of the weight loss was calculated.

Electrochemical measurements

Electrochemical experiments were conducted by use of impedance equipment (Galvanostat/Potentiostat PGZ 100) controlled with Tacussel VoltaMaster 4 corrosion-analysis software. A conventional three-electrode cylindrical Pyrex glass cell was used. The temperature was thermostatically controlled. The working electrode was C38 steel with the surface area of 1 cm^2. A saturated calomel electrode (SCE) was used as reference. The counter electrode was a platinum plate of surface area 1 cm^2.

For polarization curves, the working electrode was immersed in test solution for 30 min or until a steady-state open circuit potential (E_{ocp}) was obtained. The polarization curve was recorded by polarization from −800 to −200 mV/SCE with a scan rate of 1 mV s^{-1}. AC impedance measurements were performed in the frequency range 100 kHz–10 mHz, with 10 points per decade, at the rest potential, after immersion in acid for 30 min, by applying 10 mV ac voltage peak-to-peak. Nyquist plots were obtained from these experiments. To produce the Nyquist plot, the data points were fitted to the best semicircle, by use of a non-linear least square fit, to give the intersections with the *x*-axis.

Results and discussion

Weight loss measurements

The effect of addition of BNPP at different concentrations on the corrosion of C38 steel in 1 M HCl solution was studied by measurement of weight loss at 298 K after immersion for 6 h. From the values of the rate of corrosion in the absence (W_u) and presence (W_i) of inhibitor, the inhibition efficiency, E_G (%), was determined by use of the equation:

$$E_G\% = \frac{W_u - W_i}{W_u} \times 100 \quad (1)$$

It is obvious from the Table 1 that BNPP inhibits the corrosion of C38 steel in 1 M HCl solution at all the concentrations used in this study. The rate of corrosion

(W) decreased continuously with increasing additive concentration at 298 K. The rate of corrosion of C38 steel decreased with increasing inhibitor concentration and E_G (%) values for BNPP increased with increasing concentration. The maximum E_G (%) of 90 % was achieved at 10^{-3} M.

It should be noted that organic compounds are known to yield unreliable and irreproducible results for concentrations higher than 2×10^{-2} M [28–30]. For this reason, in this present test concentrations were up to 10^{-3} M only.

Inhibition of corrosion of C38 steel by BNPP can be explained on the basis of adsorption on the metal surface. This compound can be adsorbed on the metal surface by interaction between the metal surface and lone pairs of electrons of nitrogen and oxygen atoms and the π-electrons of the heterocyclic structure of the inhibitor [31]. This process is facilitated by the presence of vacant orbitals of low energy in iron atoms, as observed for other transition group metals [32, 33].

Polarization measurements

Polarization measurements were conducted to obtain knowledge about the kinetics of the anodic and cathodic reactions. Polarization curves for C38 steel in 1 M HCl solutions without and with addition of different concentrations of BNPP at 298 K are shown in Fig. 2. The anodic and cathodic current–potential curves were extrapolated to their intersection at a point where corrosion current density (I_{corr}) and corrosion potential (E_{corr}) are obtained. Table 2 shows the electrochemical data (I_{corr}, E_{corr}, b_a, and b_c) obtained from Tafel plots for the C38 steel electrode in 1 M HCl solution without and with different concentrations of BNPP. The I_{corr} values were used to calculate the inhibition efficiency, E_I (%) (listed in Table 2), by use of the equation:

$$E_I\% = \frac{I_u - I_i}{I_u} \times 100 \quad (2)$$

where I_u and I_i are the corrosion current densities for the C38 steel electrode in the uninhibited and inhibited solutions, respectively.

From Fig. 2 it can be seen that with increasing BNPP concentration both anodic and cathodic currents were inhibited. This result shows that addition of BNPP reduces anodic dissolution and also retards the hydrogen-evolution reaction. The Tafel lines in Fig. 2 were almost parallel when inhibitor concentration was increased, suggesting the inhibitor acted by simple blocking of the C38 steel surface [34]. In other words, the inhibitor reduced the surface area available for corrosion

Table 1 Corrosion data obtained from measurement of weight loss of C38 steel in 1 M HCl containing different concentrations of BNPP at 298 K

Conc. (M)	W_{corr} (mg/cm^2 h)	E_G (%)
Blank	1.00	–
10^{-3}	0.10	90.00
10^{-4}	0.18	82.00
10^{-5}	0.23	77.00
10^{-6}	0.29	71.00

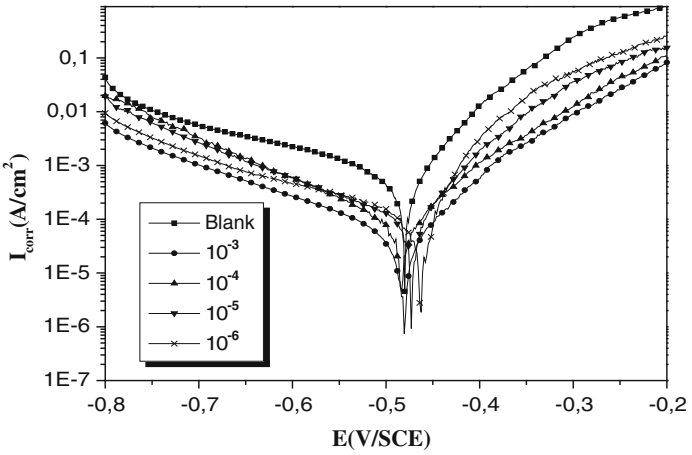

Fig. 2 Potentiodynamic polarisation curves for steel in 1 M HCl in the presence of different concentrations of BNPP

Table 2 Electrochemical data for C38 steel in 1 M HCl containing different concentrations of BNPP, and the corresponding inhibition efficiency

Conc. (M)	$-E_{corr}$ (mV/SCE)	I_{corr} (μA/cm^2)	$-b_c$ (mV/dec)	E_I (%)
Blank	480	355	189	–
10^{-3}	479	39	161	89.01
10^{-4}	482	74	137	79.15
10^{-5}	472	95	142	73.24
10^{-6}	463	120	188	66.19

and did not change the mechanism of either C38 steel dissolution or hydrogen evolution.

Table 2 showed that the largest displacement of the corrosion potential (E_{corr}) was about 19 mV. Only when the change in E_{corr} is not <85 mV can it be regarded as evidence that a compound is an anodic or cathodic-type inhibitor [35]. Therefore, it can be understood from the E_{corr} variation that the this compound acts as mixed-type inhibitor, and its E_I % increased with concentration. At a concentration of 10^{-3} M, the compound had good inhibition efficiency of approximately 89 % and acts as an excellent inhibitor of hydrochloric acid. The results indicated that the increase in inhibitor efficiency with concentration might be attributed to formation of a barrier film, because of adsorption of the compound on the C38 steel surface, which prevents the acid from attacking the metal surface.

EIS measurements

Impedance measurements of the C38 steel electrode at its open circuit potential after immersion for 0.5 h in 1 M HCl solution with and without BNPP inhibitor were performed over the frequency range from 100 kHz to 10 mHz. Figure 3 shows the

Nyquist plots obtained for C38 steel in 1 M HCl solution in the absence and presence of different concentrations of BNPP. Inspection of these plots reveals that each impedance diagram consists of a large capacitive loop at high frequency (HF) with one capacitive time constant. As is usual in EIS studies, the HF capacitive loop is related to the charge-transfer process occurring during metal corrosion and the double-layer behaviour [36].

Quantitative analysis of the electrochemical impedance plots was based on a physical model of the corrosion process with hydrogen depolarization and with charge transfer as the controlling step. The simplest model includes charge-transfer resistance (R_t) in parallel with the capacitance (C_{dl}) connected to the solution resistance (R_s). The equivalent circuit model used for this system is presented in Fig. 4.

It should be noted that the solid electrode is inhomogeneous on both the microscopic and macroscopic scale and corrosion is a uniform process with fluctuating active and inactive domains in which anodic and cathodic reactions occur at the corroding surface. The size and distribution of these domains depend on the degree of surface inhomogeneity. Inhomogeneities may also arise from adsorption phenomena, formation of porous and non-porous layers by passivation by the coating [28, 29, 37], and frequency dispersion [38]. This explains why the Nyquist diagrams are not perfect semicircles.

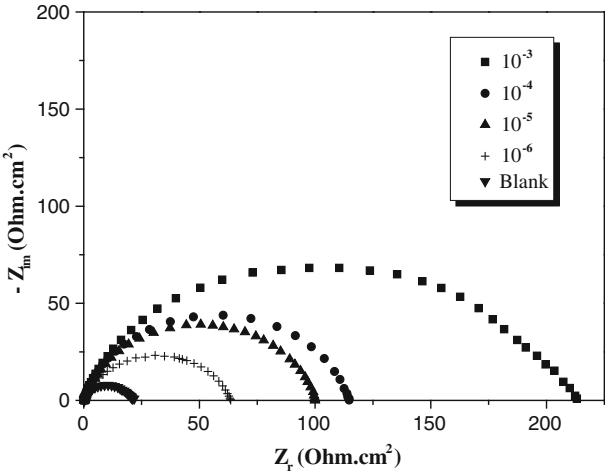

Fig. 3 Nyquist diagrams for C38 steel electrode with and without BNPP at E_{corr} after immersion for 30 min

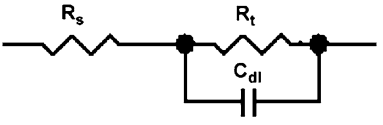

Fig. 4 The electrochemical equivalent circuit used to fit the impedance spectra

Values of the double-layer capacitance C_{dl} were calculated from the frequency at which the impedance imaginary component −Zi is maximum, by use of the equation:

$$f(-Z_{i\max}) = \frac{1}{2\pi C_{dl} R_t} \tag{3}$$

Percentage inhibition, E_{Rt} (%), was calculated from the charge-transfer resistance obtained from Nyquist plots, by use of the equation:

$$E_{Rt}(\%) = \frac{R_t' - R_t}{R_t'} \times 100 \tag{4}$$

where R_t and R_t' are the values of the charge-transfer resistance without and with inhibitor, respectively.

Table 3 gives the values of the charge-transfer resistance R_t, the double-layer capacitance C_{dl}, and the inhibition efficiency obtained from these plots. It can be seen that the presence of BNPP enhances the values of R_t and reduces C_{dl} values. The decrease in C_{dl}, which can result from a decrease in local dielectric constant and/or an increase in the thickness of the electric double layer [39], suggested that the BNPP molecules function by adsorption at the metal–solution interface. Thus, the decrease in C_{dl} values and the increase in R_t values and, consequently, inhibition efficiency may be because of gradual replacement of water molecules (the volume of a water molecule is 27.19 $Å^3$) by adsorption of BNPP molecules on the metal surface, reducing the extent of the dissolution reaction [40, 41]. Results based on impedance measurements were in good agreement with those based on weight loss and polarization curves.

Adsorption isotherm

It is widely acknowledged that adsorption isotherms provide useful insights into the mechanism of corrosion inhibition. The surface coverage, θ, was calculated by use of the equation:

$$\theta = \frac{W_u - W_i}{W_u} \tag{5}$$

The surface coverage values (θ) for different concentrations of the inhibitor were obtained from weight loss measurements at 298 K. To use corrosion rate

Table 3 Electrochemical impedance data for corrosion of C38 steel in acid medium containing different concentrations of BNPP

Conc. (M)	R_t (Ω cm^2)	f_{max} (Hz)	C_{dl} (μF/cm^2)	E_{Rt} (%)
Blank	21	89	85.19	–
10^{-3}	213	20	37.38	90.14
10^{-4}	115	25	55.39	81.74
10^{-5}	100	32	49.76	79.00
10^{-6}	63	40	63.19	66.66

measurements to evaluate thermodynamic data pertaining to inhibitor adsorption it is necessary to determine empirically which adsorption isotherm best fits the surface coverage data. We supposed that adsorption of this inhibitor followed the Langmuir adsorption isotherm:

$$\theta = \frac{\mathrm{KC}}{\mathrm{KC} + 1} \tag{6}$$

where K is the adsorption coefficient:

$$K = \left(\frac{1}{55.5}\right) \exp\left(-\frac{\Delta G_{\mathrm{ads}}}{\mathrm{RT}}\right) \tag{7}$$

The best-fit straight line was obtained for the plot of C/θ versus C; the slope was very close to 1. The strong correlation ($r^2 > 0.999$) suggested that adsorption of the inhibitor on the metal surface obeyed the Langmuir adsorption isotherm (Fig. 5).

From the intercepts of the straight lines on the C/θ-axis, the K value can be calculated. It is related to the standard free energy of adsorption ΔG_{ads}. The values of K, slope, regression factors, and $\Delta G^{\circ}_{\mathrm{ads}}$ obtained are summarized in Table 4.

The negative values of ΔG_{ads} show that adsorption of BNPP is a spontaneous process [6, 42] under the experimental conditions described. It is well known that values of $-\Delta G_{\mathrm{ads}}$ of the order of 20 kJ/mol or lower are indicative of physisorption; values 40 kJ/mol or higher involve charge sharing or transfer from the inhibitor molecules to the metal surface to form co-ordination type bonds [8, 43, 44]. Accordingly, the value of $-\Delta G_{\mathrm{ads}} = -40.62$ kJ/mol suggests chemisorption of BNPP molecules on the C38 steel surface. In fact, because of strong adsorption of

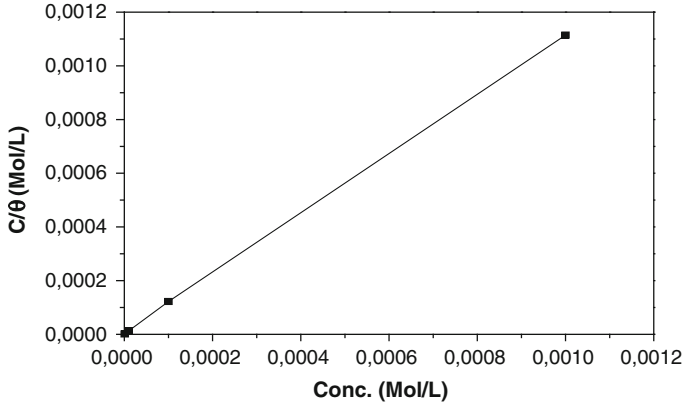

Fig. 5 Langmuir adsorption plot for C38 steel in 1 M HCl containing different concentrations of BNPP

Table 4 Thermodynamic data for of C38 steel in 1 M HCl in the absence and presence of different concentrations of BNPP

Slope	K_{ads} (M^{-1})	R^2	ΔG_{ads} (kJ/Mol)
1.1	2.39×10^5	0.99	−40.62

water molecules on the surface of C38 steel, it may be assumed that removal of water molecules from the surface is accompanied by chemical interaction between the metal surface and the adsorbate [45, 46].

Effect of temperature

To investigate the mechanism of inhibition and to calculate the activation energies of the corrosion process, EIS measurements were obtained at different temperatures in the absence and the presence of BNPP. Figures 6 and 7 give the Nyquist plots for C38 steel in the absence and presence of 10^{-3} M BNPP at different temperatures.

The corresponding data are given in Table 5. In the temperature range studied (298–328 K) the values of R_t decrease with increasing temperature both in uninhibited and inhibited solutions and efficiency of inhibition by BNPP decreases with increasing temperature. The R_t value of C38 steel increases more rapidly with temperature in the presence of the inhibitor; these results confirm that BNPP acts as an efficient inhibitor in the range of temperature studied.

The activation data for the corrosion process were calculated from the Arrhenius-type plot by use of the equation:

$$\ln\left(\frac{1}{R_t}\right) = -\frac{E_a}{RT} + \log A \tag{8}$$

where E_a is the apparent activation energy, A the pre-exponential factor, R the universal gas constant, and T the absolute temperature.

Variation of logarithm of $1/R_t$ for C38 steel in HCl containing 10^{-3} M BNPP with the reciprocal of the absolute temperature is presented in Fig. 8. Straight lines with correlation coefficients >0.98 were obtained.

Calculated values of the apparent activation energy for corrosion in the absence and presence of BNPP are listed in the Table 6. The value of E_a found for BNPP is higher

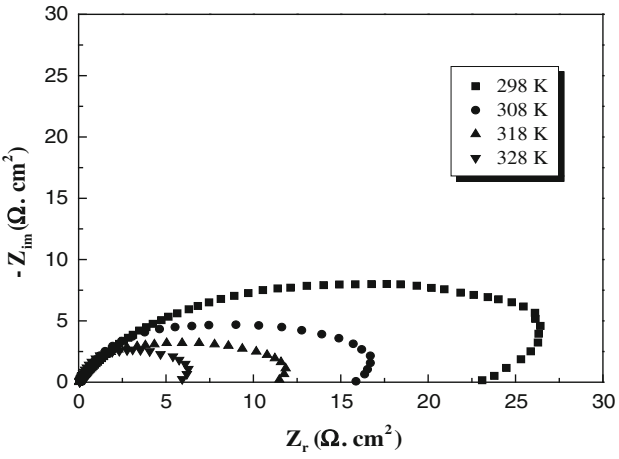

Fig. 6 Nyquist diagrams for C38 steel in 1 M HCl at different temperatures

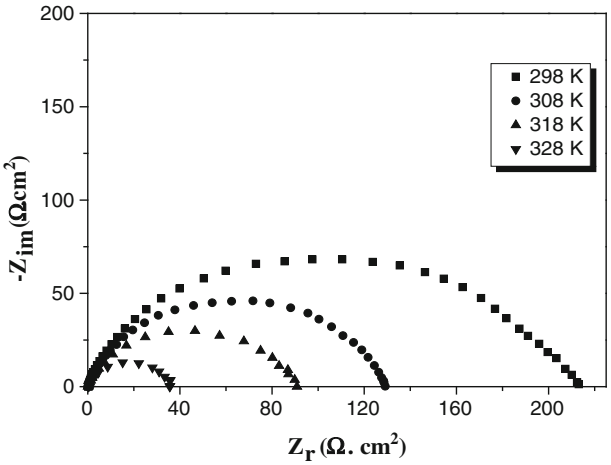

Fig. 7 Nyquist diagrams for C38 steel in 1 M HCl + 10^{-3} M BNPP at different temperatures

Table 5 Thermodynamic data for adsorption of BNPP in 1 M HCl on C38 steel at different temperatures

Temp. (K)	R_t (Ω cm^2)	f_{max} (Hz)	C_{dl} (μF/cm^2)	E_{Rct} (%)
Blank				
298	21	89	85.19	–
308	13	152	80.58	–
318	10	244	65.26	–
328	5.4	588	50.15	–
BNPP				
298	213	20	37.37	90.14
308	129	25	49.37	89.92
318	90	30	58.33	88.88
328	35	50	90.99	84.57

than that obtained for 1 M HCl solution. The increase in the apparent activation energy may be interpreted on the basis of physical adsorption occurring in the first stage [47]. Szauer and Brand [48] explained that the increase in activation energy can be attributed to an appreciable decrease in adsorption of the inhibitor on the C38 steel surface with increasing temperature. As adsorption decreases, more desorption of inhibitor molecules occurs because these two opposing processes are in equilibrium. Because of increasing desorption of inhibitor molecules at higher temperatures, more of the surface of the C38 steel comes into contact with the aggressive environment, resulting in an increased rate of corrosion with increasing temperature [49].

An alternative formulation of Arrhenius equation is [50]:

$$1/R_t = \frac{RT}{Nh} \exp\left(\frac{\Delta S_a^*}{R}\right) \exp\left(\frac{\Delta H_a^*}{RT}\right) \quad (9)$$

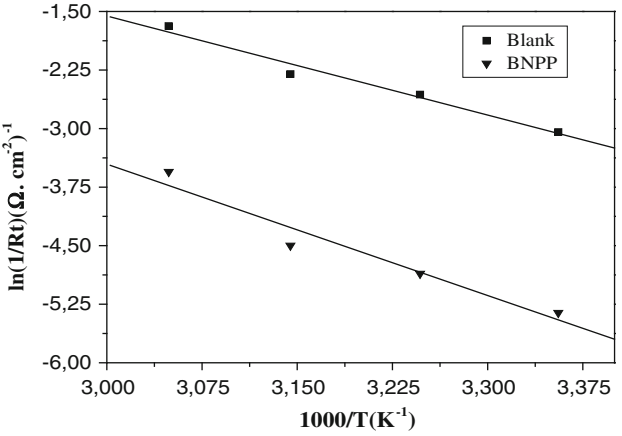

Fig. 8 Arrhenius plots for C38 steel in 1 M HCl with and without 10^{-3} M BNPP

Table 6 Activation data E_a, ΔH_a, ΔS_a, and ΔG_{ads} for C38 steel in 1 M HCl in the absence and presence of 10^{-3} M BNPP

	E_a (kJ/mol)	ΔH_a (kJ/mol)	ΔS_a (J/mol)	$E_a - \Delta H_a$ (kJ/mol)
Blank	35.13	32.54	−161.04	2.59
BNPP	46.58	43.98	−142.48	2.60

where h is Planck's constant, N is Avogadro's number, $\Delta S_a^*$is the entropy of activation and ΔH_a^* is the enthalpy of activation. Figure 9 shows a plot of Ln ($1/R_t$·T) against 1/T. Straight lines are obtained with a slope of $\frac{\Delta H_a^*}{R}$ and an intercept of Ln R/Nh $+\frac{\Delta S_a^*}{R}$ from which the values of ΔS_a^* and ΔH_a^* are calculated; these are given in Table 6.

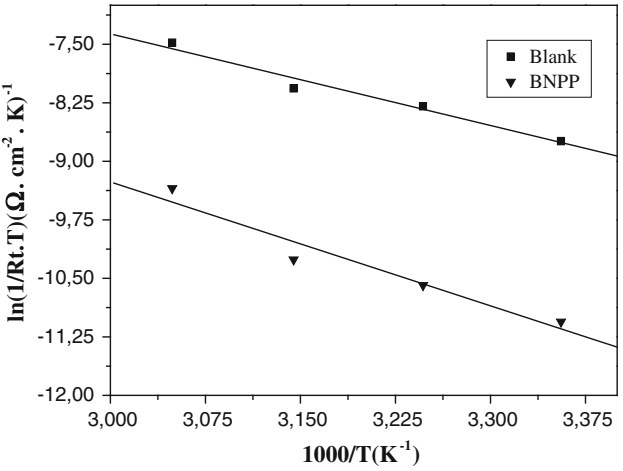

Fig. 9 Arrhenius plots for C38 steel in 1 M HCl with and without 10^{-3} M BNPP

Inspection of these data revealed that the thermodynamic data (ΔH_a^* and ΔS_a^*) for dissolution reaction of C38 steel in 1 M HCl in the presence of inhibitor are higher than those obtained in the absence of inhibitor. The positive sign of ΔH_a^* reflects the endothermic nature of the C38 steel dissolution process, suggesting that dissolution of C38 steel is slow [51] in the presence of inhibitor. On comparing the values of the entropy of activation ΔS_a^* given in Table 6, it is clear that entropy of activation decreases more negatively in the presence of BNPP than in the absence of inhibitor; this reflects the formation of an ordered stable layer of inhibitor on the C38 steel surface [52].

We remark that E_a and ΔH_a^*values vary in the same way (Table 6). This result enables verification the known thermodynamic relationship between the E_a and ΔH_a^* as shown in Table 5 [8]:

$$E_a - \Delta H_a^* = RT \tag{10}$$

Conclusion

The following conclusions can be drawn from this study:

- The inhibiting effect of BNPP increases with increasing inhibitor concentration and reached a maximum at 10^{-3} M.
- Polarization study showed that the compound under investigation was mixed type inhibitor.
- Results from weight loss, electrochemical impedance spectroscopy, and polarisation curves were in good agreement.
- Adsorption of BNPP on the C38 steel surface from 1 M HCl followed the Langmuir isotherm.
- The efficiency of inhibition by BNPP decreased with increasing temperature and its addition led to a increase of the activation energy for corrosion.

References

1. N.O. Eddy, E.E. Ebenso, Afri. J. Pure Appl. Chem. **2**, 46 (2008)
2. N.O. Eddy, S.A. Odoemelam, Mat. Sci. (India) **4**, 9 (2008)
3. L. Larabi, Y. Harek, O. Benali, S. Ghalem, Prog. Org. Coat. **54**, 256 (2005)
4. O. Benali, L. Larabi, S. Merah, Y. Harek, J. Mater. Environ. Sci. **2**(1), 39 (2011)
5. L. Larabi, O. Benali, Y. Harek, Port. Electrochim. Acta. **24**, 337 (2006)
6. O. Benali, L. Larabi, B. Tabti, Y. Harek, Anti-Corros. Met. Mat. **52**, 280 (2005)
7. L. Larabi, O. Benali, S.M. Mekelleche, Y. Harek, Appl. Surf. Sci. **253**, 1371 (2006)
8. O. Benali, L. Larabi, M. Traisnel, L. Gengenbre, Y. Harek, Appl. Surf. Sci. **253**, 6130 (2007)
9. O. Benali, M. Ouazene, Arab. J. Chem. **4**, 443 (2011)
10. H.B. Ouici, O. Benali, Y. Harek, L. Larabi, B. Hammouti, A. Guendouzi, Res. Chem. Intermed. doi 10.1007/s11164-012-0797-1
11. M. Mihit, R. Salghi, S. El Issami, L. Bazzi, B. Hammouti, E. Ait Addi, S. Kertit, Pig. Res. Tech. **35**, 151 (2006)
12. A. Dafali, B. Hammouti, R. Mokhlisse, S. Kertit, Corros. Sci. **45**, 1619 (2003)

13. H. Zarrok, H. Oudda, A. Zarrouk, R. Salghi, B. Hammouti, M. Bouachrine, Der Pharm. Chem. **3**, 576 (2011)
14. S. Kertit, R. Salghi, L. Bazzi, B. Hammouti, A. Bouchtart, Ann. Chim. Sci. Mat. **25**, 187 (2000)
15. M. Mihit, K. Laarej, H. Abou El Makarim, L. Bazzi, R. Salghi, B. Hammouti, Arab. J. Chem. **3**, 55 (2010)
16. H. Zarrok, A. Zarrouk, B. Hammouti, R. Salghi, C. Jama, F. Bentiss, Corros. Sci. **64**, 243 (2012)
17. K. Barouni, L. Bazzi, R. Salghi, M. Mihit, B. Hammouti, A. Albourine, S. El Issami, Mater. Lett. **62**, 3325 (2008)
18. S. El Issami, L. Bazzi, M. Mihit, B. Hammouti, S. Kertit, E. Ait Addi, R. Salghi, Pig. Res. Tech. **36**, 161 (2007)
19. S. El Issami, L. Bazzi, M. Mihit, M. Hilali, R. Salghi, E. Ait Addi, J. Phys. IV **123**, 307 (2005)
20. M. Mihit, S. El Issami, M. Bouklah, L. Bazzi, B. Hammouti, E. Ait Addi, R. Salghi, S. Kertit, Appl. Surf. Sci. **252**, 2389 (2006)
21. H. Bendaha, A. Zarrouk, A. Aouniti, B. Hammouti, S. El Kadiri, R. Salghi, R. Touzani, Phys. Chem. News. **64**, 95 (2012)
22. A. Zarrouk, H. Zarrok, R. Salghi, N. Bouroumane, B. Hammouti, S.S. Al-Deyab, R. Touzani, Int. J. Electrochem. Sci. **7**, 10215 (2012)
23. S. El Issami, L. Bazzi, M. Hilali, R. Salghi, S. Kertit, Ann. Chim. Sci. Mat. **27**, 63 (2002)
24. H. Zarrok, A. Zarrouk, R. Salghi, Y. Ramli, B. Hammouti, M. Assouag, E.M. Essassi, H. Oudda, M. Taleb, J. Chem. Pharm. Res. **4**(12), 5048 (2012)
25. R. Salghi, L. Bazzi, B. Hammouti, S. Kertit, Bull. Electrochem. **16**, 272 (2000)
26. B. Hammouti, R. Salghi, S. Kertit, J. Electrochem. Soc. India **47**, 31 (1998)
27. A. Zarrouk, B. Hammouti, H. Zarrok, R. Salghi, M. Bouachrine, F. Bentiss, S.S. Al-Deyab, Res. Chem. Intermed. **38**, 2327 (2012)
28. B. Donnelly, T.C. Downie, R. Grzeskowiak, H.R. Hamburg, D. Short, Corros. Sci. **18**, 109 (1978)
29. H. Zarrok, A. Zarrouk, R. Salghi, M. Assouag, B. Hammouti , H. Oudda, S. Boukhris , S. S. Al Deyab, I. Warad, Der Pharmacia Lettre. **5**(2), 43 (2013)
30. K.F. Khaled, A. El-Maghraby, Arab. J. Chem. doi:10.1016/j.arabjc.2010.11.005
31. F. Xu, B. Hou, Acta Metall. Sin. (Engl. Lett.) **22**(4), 247 (2009)
32. O. Benali, H. Benmehdi, O. Hasnaoui, C. Selles, R. Salghi, J. Mater. Environ. Sci. **4**(1), 127 (2013)
33. H.B. Ouici, O. Benali, Y. Harek, L. Larabi, B. Hammouti, A. Guendouzi, Res. Chem. Intermed. doi 10.1007/s11164-012-0821-5
34. Y. Abboud, A. Abourriche, T. Saffaj, M. Berrada, Appl. Surf. Sci. **252**, 8178 (2006)
35. H. Ashassi-Sorkhabi, M.R. Majidi, K. Seyyedi, Appl. Surf. Sci. **225**, 176 (2004)
36. D. Ben Hmamou, R. Salghi, A. Zarrouk, O. Benali, F. Fadel, H. Zarrok, B. Hammouti, Int. J. Ind. Chem. **3**, 25 (2012)
37. Z.B. Stoynov, B.M. Grafov, B. Savova-Stoynova, V.V. Elkin, *Electrochemical Impedance* (Nauka, Moscow, 1991)
38. F. Mansfeld, M.W. Kendig, S. Tsai, Corrosion **38**(3), 130 (1982)
39. E. McCafferty, N. Hackerman, J. Electrochem. Soc.**119**, 146 (1972)
40. F. Bentiss, M. Traisnel, M. Lagrenee, Corros. Sci. **42**, 127 (2000)
41. S. Muralidharan, K.L.N. Phani, S. Pitchumani, S. Ravichhandran, S.V.K. Iyer, J. Electrochem. Soc. **142**, 1478 (1995)
42. A.E. Fouda, H.A. Mostafa, H.M. Abu-Elnader, Monatshefte fur. Chem. **104**, 501 (1989)
43. F.M. Donahue, K. Nobe, J. Electrochem. Soc. **112**, 886 (1965)
44. E. Kamis, F. Belluci, R.M. Latanision, E.S.H. El-Ashry, Corrosion **47**, 677 (1991)
45. L.M. Vracar, D.M. Drazic, Corros. Sci. **44**, 1669 (2002)
46. F. Zhang, Y. Tang, Z. Cao, W. Jing, Z. Wu, Y. Chen, Corros. Sci. **61**, 1 (2012)
47. S. Martinez, I. Stern, Appl. Surf. Sci. **199**, 83 (2002)
48. T. Szauer, A. Brand, Electrochim. Acta **26**, 1219 (1981)
49. L. Afia, R. Salghi, A. Zarrouk, H. Zarrok, O. Benali, B. Hammouti, S.S. Al-Deyab, A. Chakir, L. Bazzi, Portug. Electrochim. Acta **30**(4), 267 (2012)
50. J.O.M. Bochris, A.K.N. Reddy, *Modern Electrochemistry* (Plenum Press, New York, 1977)
51. N.M. Guan, L. Xueming, L. Fei, Mater. Chem. Phys. **86**, 59 (2004)
52. A. Yurt, A. Balaban, S.U. Kandemir, G. Bereket, B. Erk, Mater. Chem. Phys. **85**, 420 (2004)